Angewandte Chemie
Eine Zeitschrift der Gesellschaft Deutscher Chemiker

Supporting Information

Optical Control of Insulin Secretion Using an Incretin Switch

Johannes Broichhagen, Tom Podewin, Helena Meyer-Berg, Yorrick von Ohlen, Natalie R. Johnston, Ben J. Jones, Stephen R. Bloom, Guy A. Rutter, Anja Hoffmann-Röder, David J. Hodson,* and Dirk Trauner**

anie_201506384_sm_miscellaneous_information.pdf

Table of Contents

1. Chemistry and Spectroscopy

1.1. General

AMPP synthesis

AMPP was synthesized as previously described[1] and spectra matched those reported.

Peptide synthesis

Peptide synthesis was performed on a CEM Liberty 1 Peptide Synthesizer with a CEM Discovery Microwave using standard Fmoc-protected solid phase peptide synthesis protocols. Detailed information to peptide synthesis, resin, coupling reagents and conditions can be found in 1.3.

Reversed-phase HPLC

Analytical RP-HPLC was performed on Jasco devices (PU- 2080 Plus, LG-2080-02-S, DG-2080-53 and MD-2010 Plus) with a Phenomenex Luna column (C18, 5 μm, 250x4.6 mm). As eluent, a water/acetonitrile gradient containing 0.1% TFA was used with a 1 mL/min flow rate. Semi-preparative RP-HPLC was performed on Jasco devices (PU-2087 Plus, LG-2080-02-S and UV-2075 Plus) with a Phenomenex Luna column (C18, 5 μm, 250x20 mm).). The same eluent was used as for RP-HPLC, but with a 20 mL/min flow rate.

NMR

NMR spectra were recorded in 35% aqueous trifluoroethanol-d_3 (TFE-d_3) on a BRUKER Avance III HD 800 instrument and calibrated to residual solvent peaks (^{1}H/^{13}C in ppm): TFE-d_3 (3.88/126.3). To prevent thermal back relaxation during long carbon and 2D experiments, **LirAzo** was pre-illuminated to obtain the *cis*-isomer and the NMR tube was equipped with a fibre optic coupled to a Polychrome V (Till Photonics) monochromator to deliver constant UV irradiation. Spectra were necessarily acquired without spinning the probe. Multiplicities are abbreviated as follows: s = singlet, d = doublet, t = triplet, q = quartet, br = broad, m = multiplet. Spectra are reported based on appearance, not on theoretical multiplicities derived from structural information.

HRMS

High-resolution electrospray ionization (ESI) mass spectra were obtained on a Varian MAT 711 MS instrument operating in either positive or negative ionization modes.

UV/Vis

UV/Vis spectra were recorded on a Varian Cary 50 Bio UV-Visible Spectrophotometer using Helma SUPRASIL precision cuvettes (10 mm light path) equipped with a Polychrome V (Till Photonics) monochromator.

CD

CD measurements were recorded on a Jasco 810 instrument with a Jasco CDF-4265 Peltier-Element and Tris buffer (50 mM, pH = 7.4) as solvent. The cuvettes

were of 1 mm thickness. For baseline correction, a pure buffer spectrum was recorded. Sample concentrations were calculated via the specific absorption at 323 nm, with $\varepsilon_{azobenzene}$ = 25,000 L $mol^{-1}cm^{-1}$. The recorded spectra were processed with Origin 8.0 and smoothed using a 30-point Savitzky-Golay-Filter

1.2. Peptide synthesis

A solid-phase Fmoc-Glycine-Wang LL resin (Novabiochem®), pre-loaded with 0.36 mmol/g amino acid, was used. The peptides were synthesized in 0.1 mmol scale with the standard coupling reagents HBTU/HOBt·H_2O 0.5 M in DMF, activated with DIPEA 2 M in NMP. Amino acids were coupled in a tenfold excess (2 M solutions) as Fmoc-protected compounds with standard residual protecting groups. Fmoc deprotection was achieved by treatment with 20% piperidine in DMF. AMPP building blocks were coupled in a 1.5-fold excess with the coupling reagents HATU/HOAt (1.5 eq.) 0.5 M in DMF activated with NMM (5 eq.) in DMF. Coupling conditions are summarized in SI Table 1. After coupling of all compounds, the resin-bound peptide was transferred into a Merrifield reactor followed by global deprotection with TFA/phenol/triisopropylsilane/H_2O (88:5:2:5) solution within 2 h. The solvent was then precipitated in 180 mL chilled diethyl ether and stored overnight at -38 °C. The precipitated peptide was centrifuged and after decantation of the solution, the residue was dried and purified with RP-HPLC to yield the desired peptides.

1.3. HPLC traces of Lira and LirAzo peptides

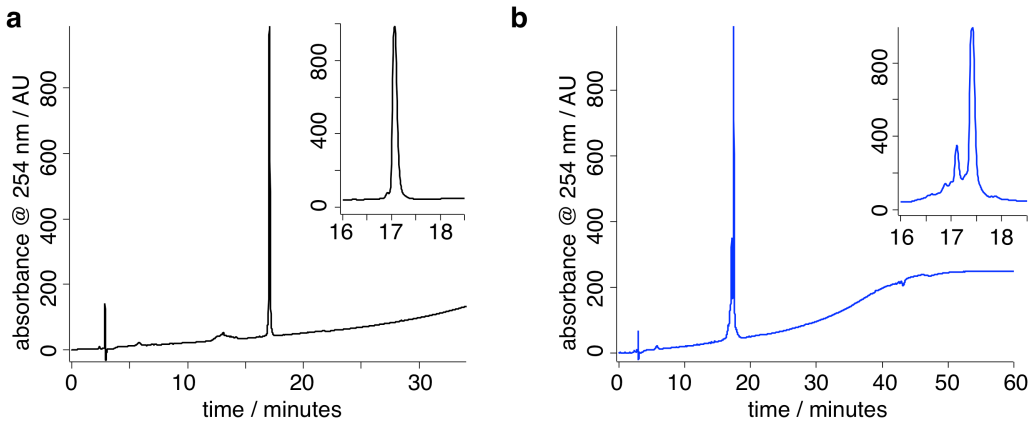

Above are analytical HPLC traces of a) Lira and b) **LirAzo** using a gradient MeCN/H2O = 10/90 → 100/0 within 40 min.

1.4. Photoswitching of LirAzo peptide

cis-/*trans*-Isomerization was assessed by UV/Vis spectroscopy following the π-π*-band (330 nm) and double-exponential fitting of the slopes (Wavemetrics Igor v6.2). τ-Values are given in Supplementary Table 1 and represented in Supplementary Figure 2.

1.5. NMR Spectra of Lira and *cis/trans*-LirAzo peptides

1.5.1. Lira

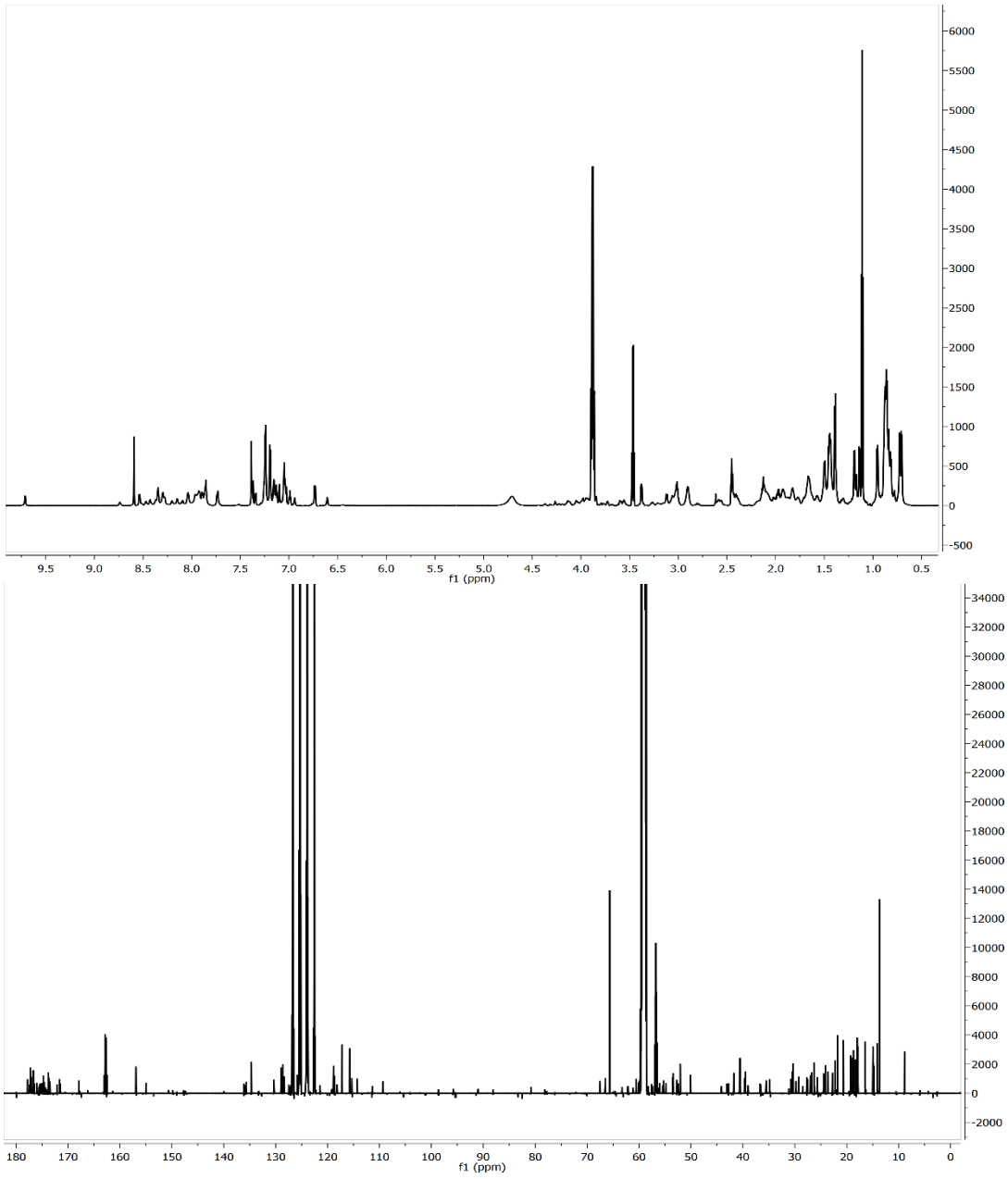

^{1}H- (top) and **^{13}C**- (bottom) NMR spectra of Lira peptide.

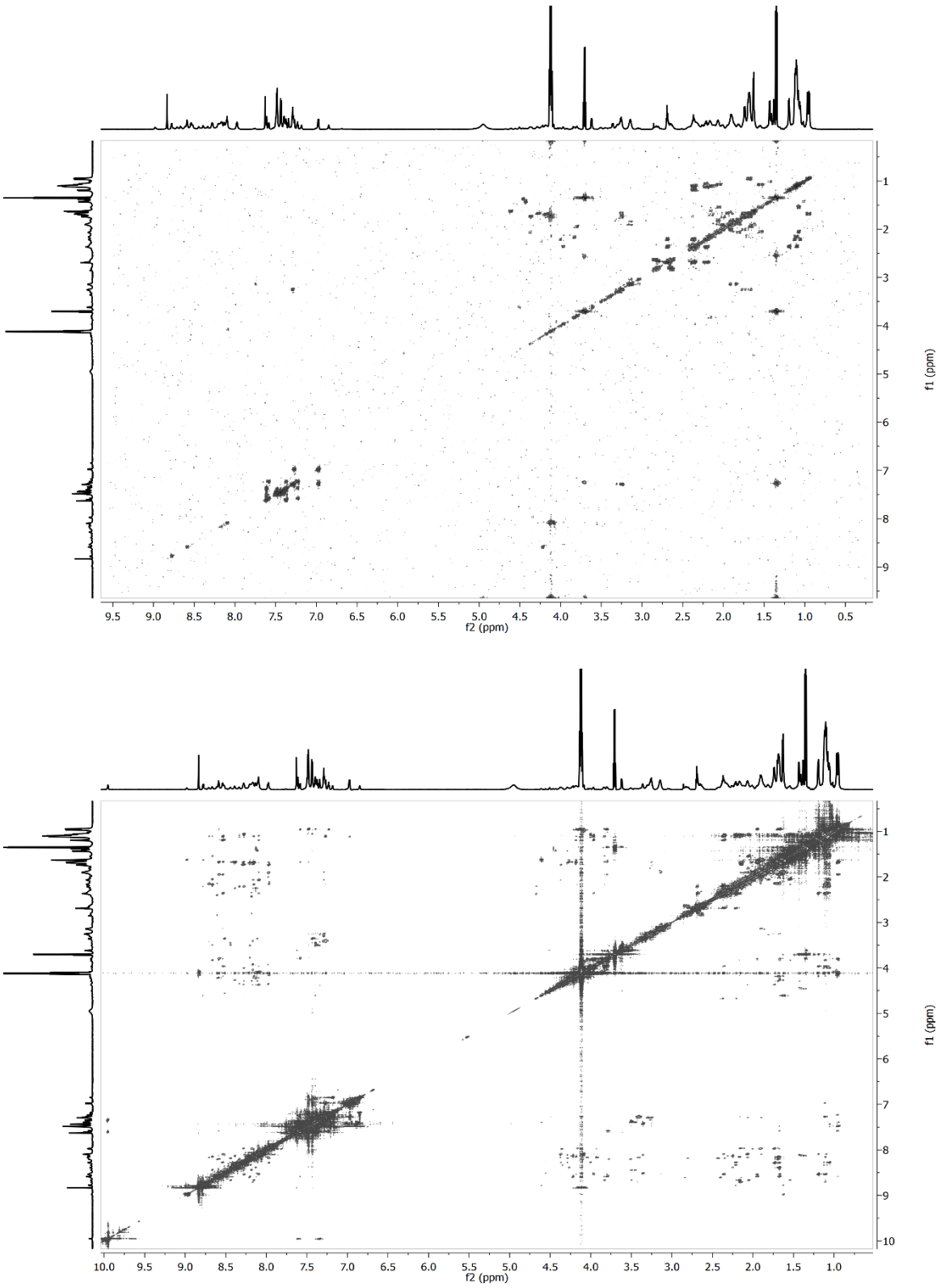

^{1}H,^{1}H-COSY (top) and **^{1}H,^{1}H-NOESY** (bottom) NMR spectra of Lira peptide.

1.5.2. *trans*-LirAzo

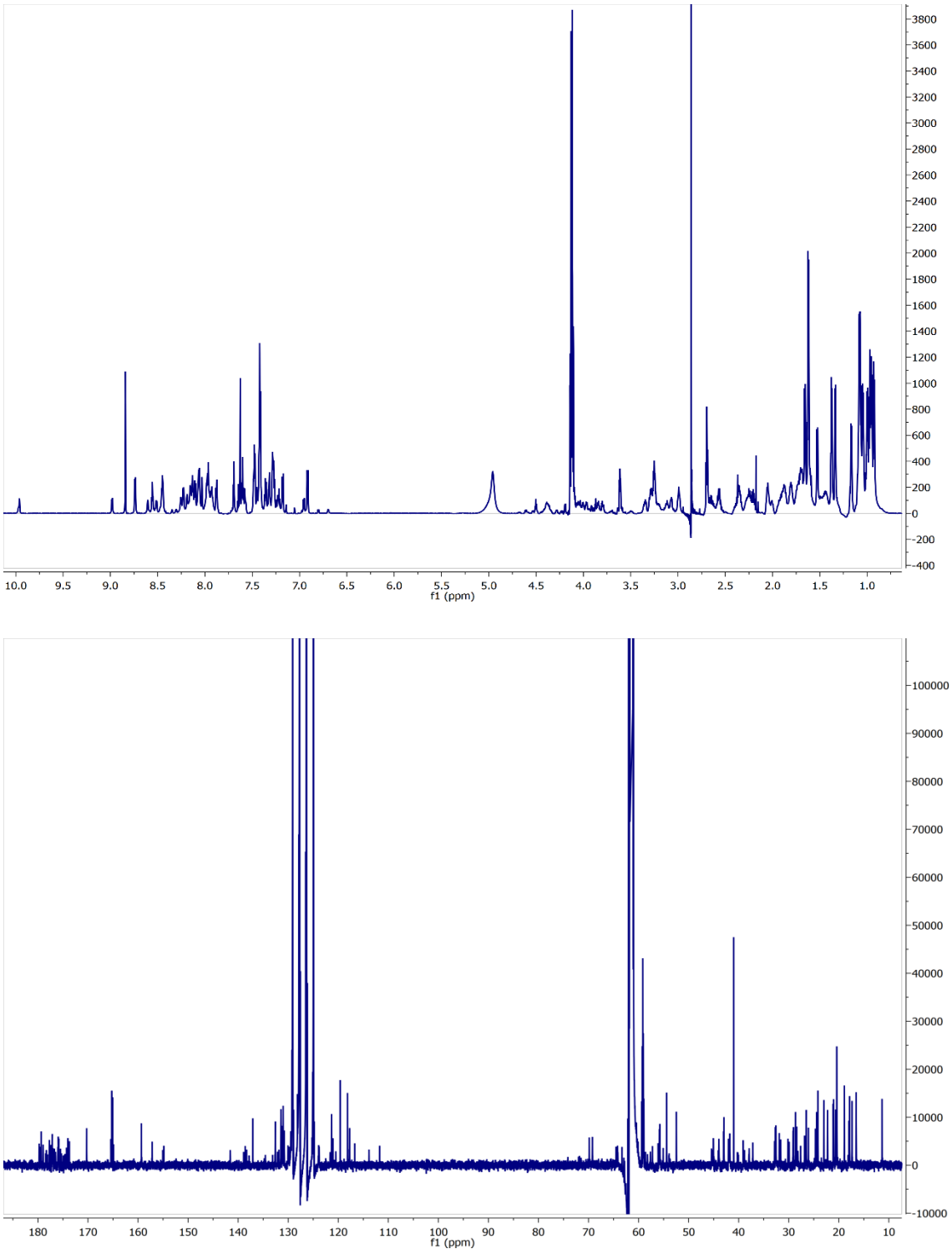

^{1}H- (top) and **^{13}C**- (bottom) NMR spectra of *trans*-**LirAzo** peptide.

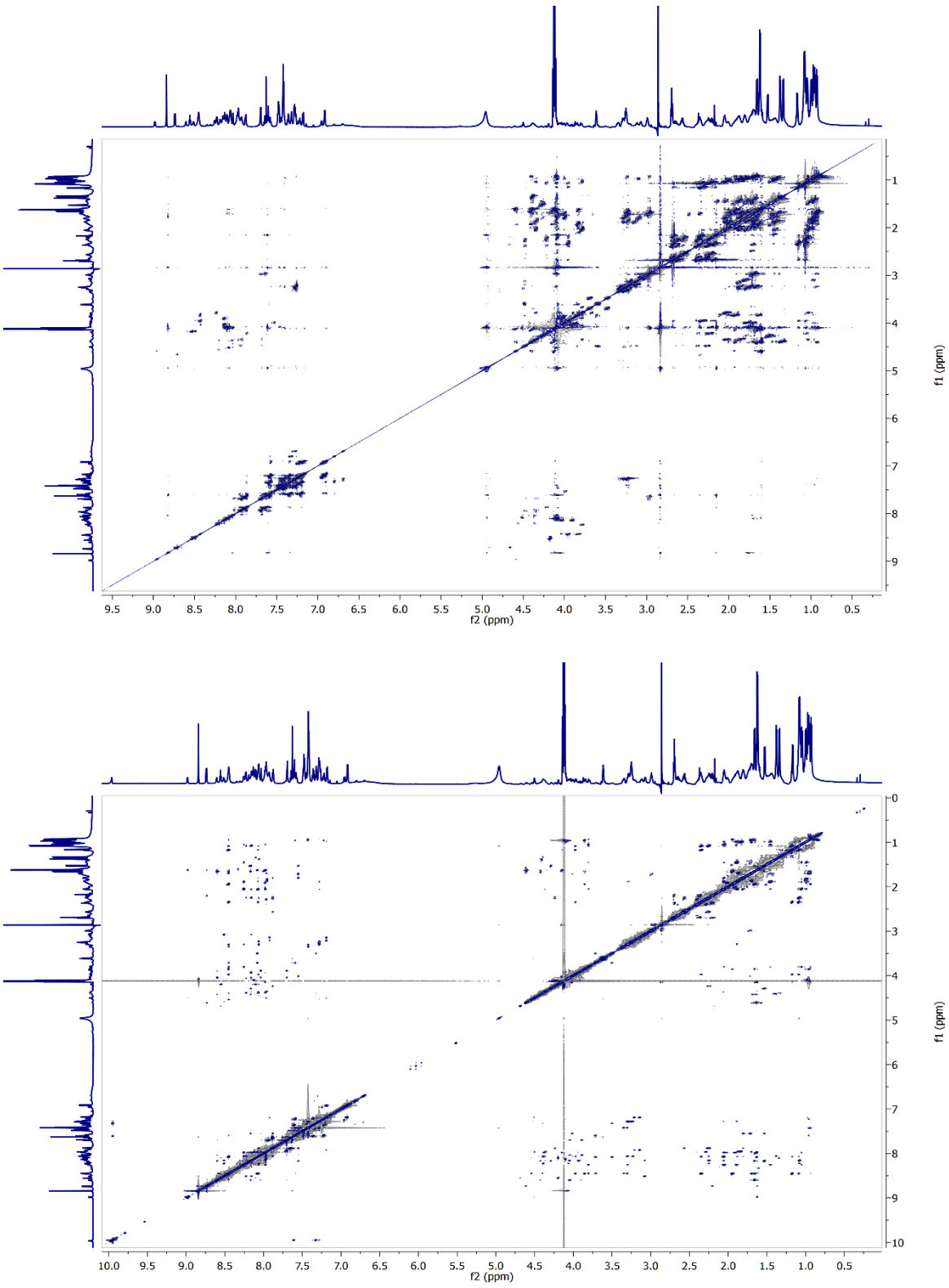

^{1}H,^{1}H-COSY (top) and **^{1}H,^{1}H-NOESY** (bottom) NMR spectra of *trans*-**LirAzo**.

1.5.3. *cis*-LirAzo

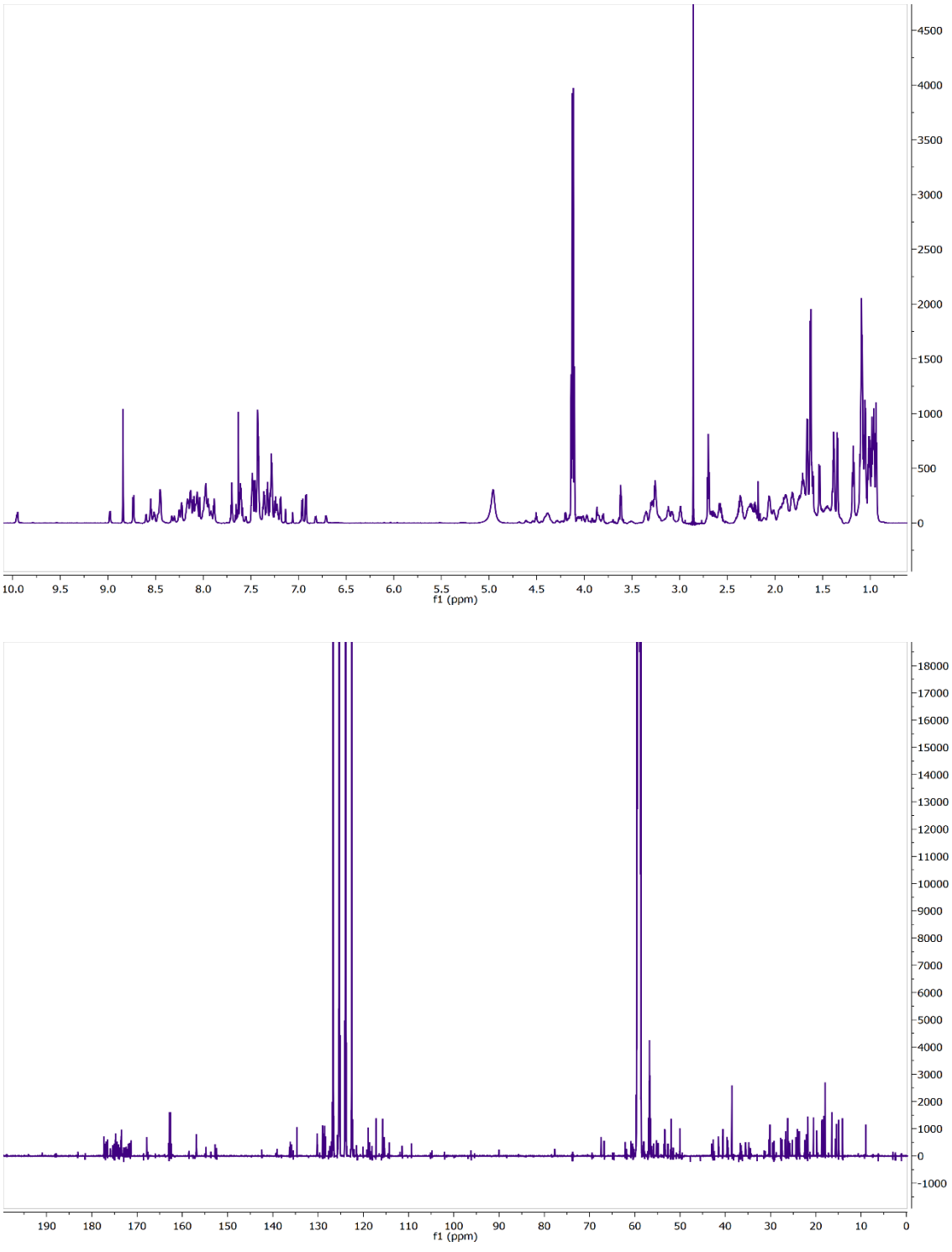

^{1}H- (top) and **^{13}C**- (bottom) NMR spectra of *cis*-**LirAzo** peptide.

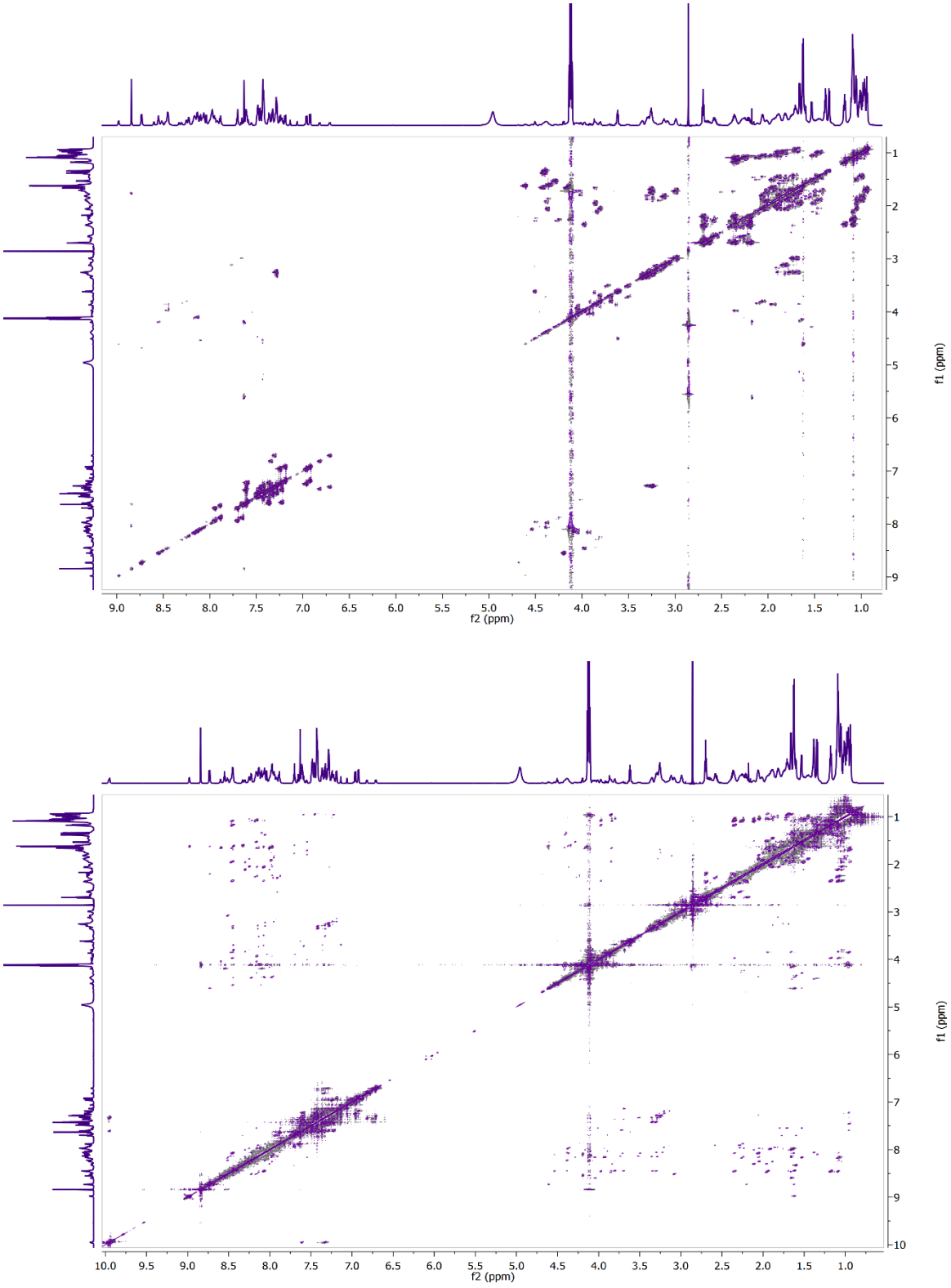

^{1}H,^{1}H-COSY **(top) and** ^{1}H,^{1}H-NOESY **(bottom)** NMR spectra of *cis*-**LirAzo**.

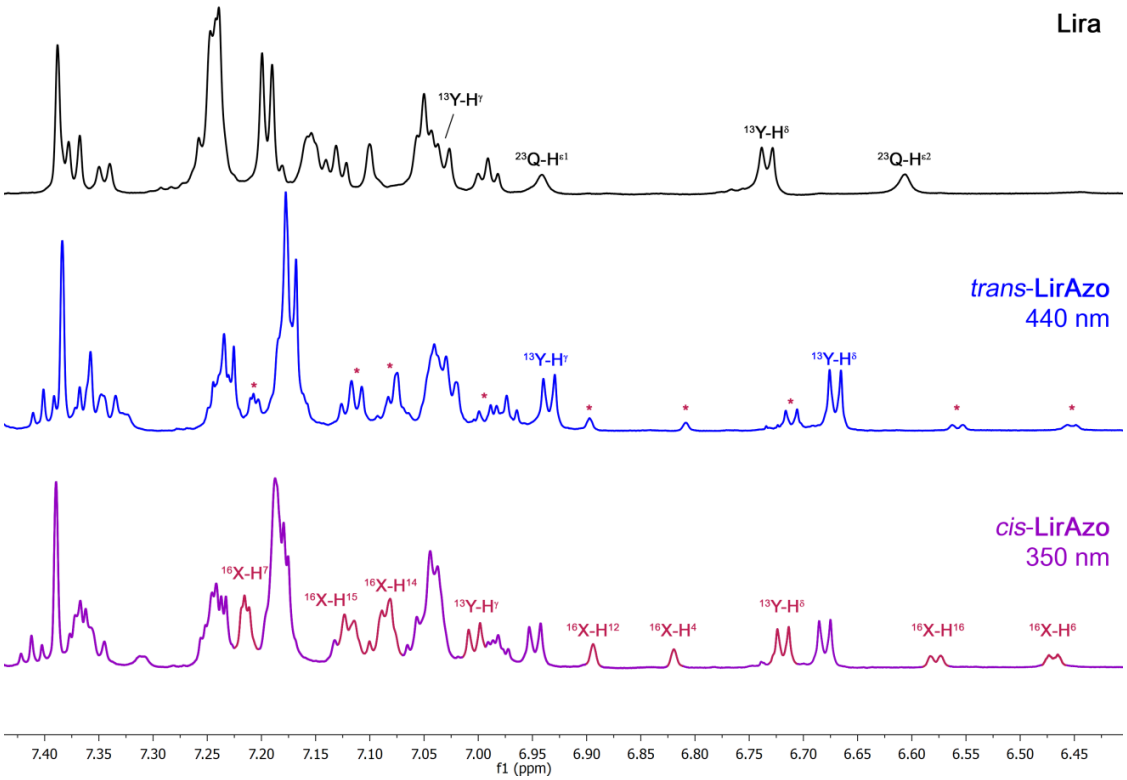

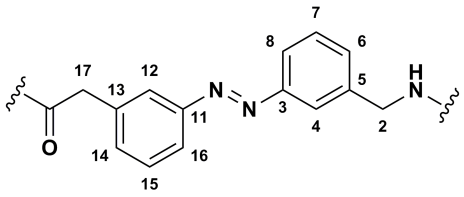

Selected aromatic signals of ^{1}H-NMR spectra of Lira (black) and *trans*-(blue)/*cis*-(purple)-**LirAzo** (top). Protons of the substituted glutamine residue (^{23}Q, black) are undetectable in *cis-/trans*-**LirAzo**. Signals emanating from AMPP (red asterisks) and tyrosine (^{19}Y-Hε doublet) become more prominent for the *cis*-isomer, demonstrating changes in secondary and tertiary structure of **LirAzo** upon isomerization. Numeration of AMPP atoms (bottom). See also Supplementary Table 3.

1.6. HRMS spectra of peptides

1.6.1. Lira

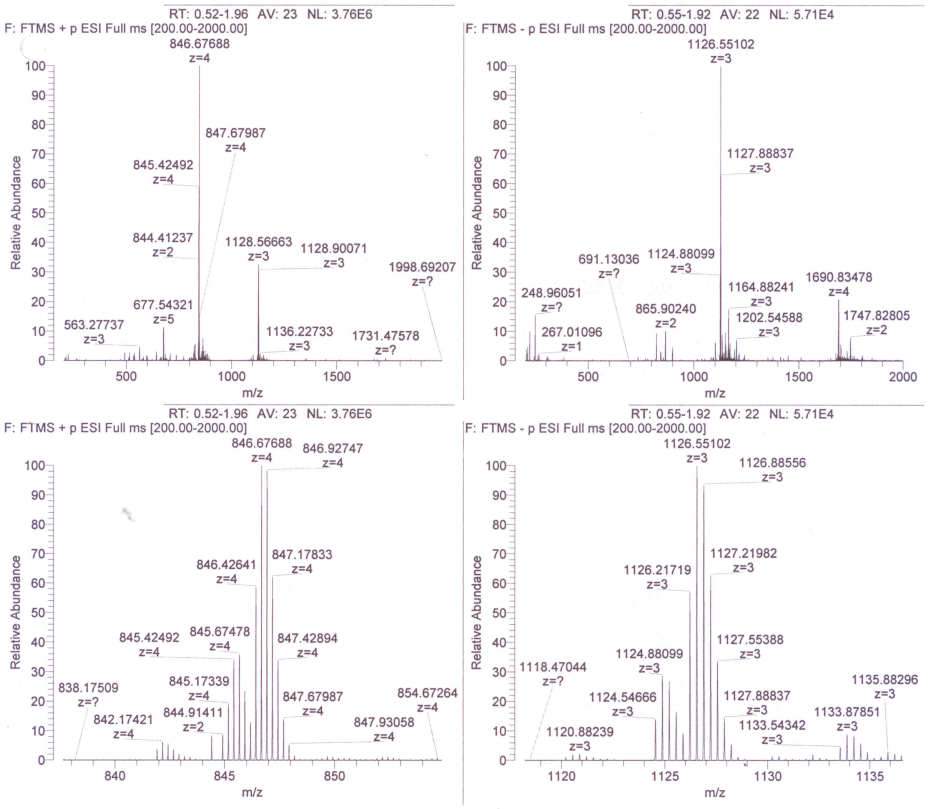

HRMS (ESI): calc. for $C_{151}H_{232}N_{42}O_{47}^{4+}$ $(M+4H)^{4+}$: 846.6767 (monoisotopic), found: 846.6769.

1.6.2. LirAzo

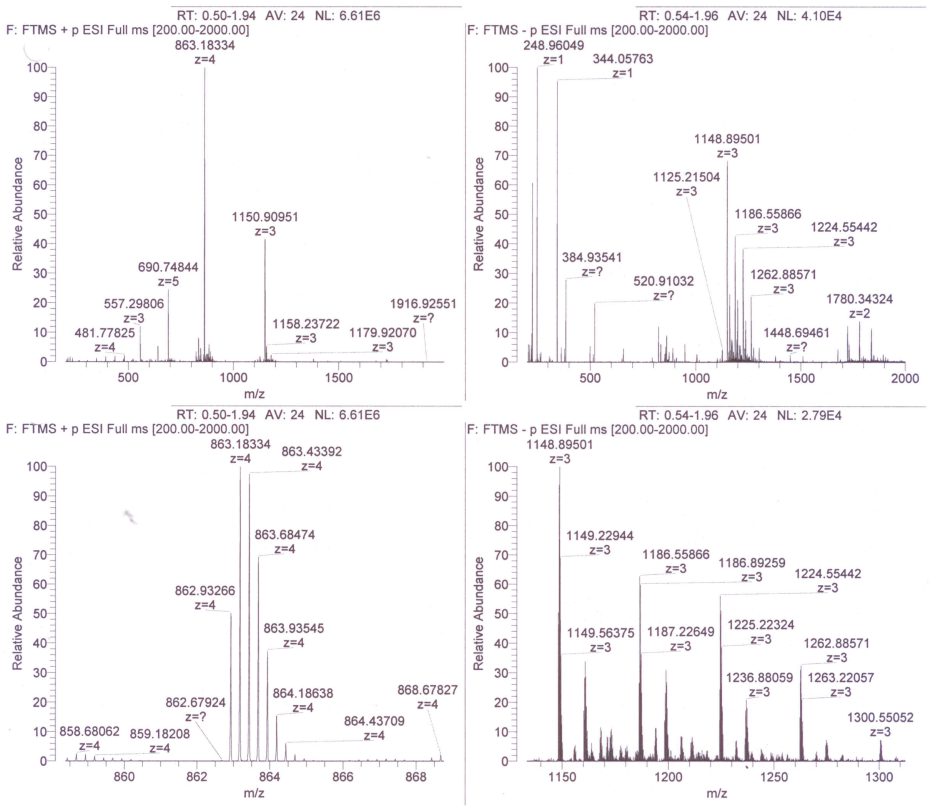

HRMS (ESI): calc. for $C_{159}H_{234}N_{42}O_{45}^{4+}$ $(M+4H)^{4+}$: 863.1831 (monoisotopic), found: 863.1833.

2. Biology

Ethical approval

All procedures involving primary tissue were regulated by the Home Office according to the Animals (Scientific Procedures) Act 1986 of the United Kingdom (PPL 70/7349).

Isolation of rodent islets

Islets were isolated from 8-12 week old female C57BL6 mice, as previously detailed,[2] and maintained in Roswell Park Memorial Institute (RPMI) medium supplemented with 10% foetal calf serum, 100 U/mL penicillin and 100 µg/mL streptomycin.

Cell lines

Chinese Hamster Ovary (CHO) cells stably expressing the GLP-1R were cultured in Dulbecco's Modified Eagle's Medium (DMEM) supplemented with 10% FBS, 1 x non-essential amino acids, 25 mM HEPES, 100 U/mL penicillin and 100 µg/mL streptomycin. MIN6 cells (a kind gift from Dr Jun-ichi Miyazaki, Osaka University) were cultured in DMEM supplemented with 15% FBS, 10 mM glutamine, 20 mM HEPES, 0.0005% β-mercaptoethanol 100 U/mL penicillin and 100 µg/mL streptomycin.

Cytotoxicity and apoptosis assays

Control, Lira and **LirAzo**-treated islets were incubated with 3 µM of calcein-AM (live) and 2.5 µM of propidium iodide (dead), and absorbance/emission detected at λ = 491/525 nm and λ = 561/620 nm, respectively. The area of dead:live cells was calculated as a ratio. Apoptosis was assessed using a DeadEnd Fluorimetric TUNEL System staining kit (Promega).[3] The apoptotic cell mass was calculated as a fraction area *versus* the total cell mass. To investigate the pro-survival effects of **LirAzo**, MIN6 beta cells were incubated for 24 hr in a glucolipotoxic mixture (33 mM glucose + 0.5 mM palmitate) in the presence or absence of compound. Apoptosis was subsequently determined using specific fluorescent immunostaining and a rabbit polyclonal antibody against cleaved caspase 3 (Cell Signaling Technology # 9661; 1:400), before analysis as above.

Calcium imaging

Multicellular Ca^{2+} imaging was performed using fluo2 and a Nipkow spinning disk confocal microscope, as detailed.[3] Briefly, pulsed λ = 491 nm light was delivered through a 10/0.3 NA objective (EC Plan-Neofluar, Zeiss) using a solid-state laser (Cobalt), and emitted signals captured from λ = 500-550 nm using a Hammamatsu ImageEM EM-CCD camera. Photoswitching was performed using either a λ = 440 nm laser or the epifluorescent port of the microscope configured with a λ = 350 ± 20 nm band-pass filter. Throughout, HEPES-bicarbonate buffer was used, containing in mM: 120 NaCl, 4.8 KCl, 24 $NaHCO_3$, 0.5 Na_2HPO_4, 5 HEPES, 2.5 $CaCl_2$ and 1.2 $MgCl_2$. Compounds and *D*-glucose were added as indicated.

cAMP and calcium assays

Cellular cAMP concentrations were determined using either Cisbio HTRF cAMP or Promega cAMP-Glo assays according to the manufacturers' instructions. Treatments were applied for 5 min before cell lysis to extract cellular cAMP. High-throughput (HTS) Ca^{2+} assays were performed using the DiscoverX HitHunter No Wash PLUS assay. Treatments were automatically delivered at 37 ^{0}C using a BMG Labtech NOVOstar platereader and fluorescence intensity read over 30-45 s. Absorbance/emission were detected at λ = 488/525 nm. For all assays, **LirAzo** was preilluminated at λ = 300-340 using a UVP 3UV benchtop transilluminator to induce *cis*-isomerization, or kept in the dark to maintain the *trans*-isomer. In addition, for HTS Ca^{2+} assays, λ = 340 ± 10 nm or λ = 450 ± 10 nm was delivered between acquisitions using the platereader's inbuilt multichromator.

Insulin secretion assays

Batches of six to eight islets were incubated for 30 min in Krebs-HEPES-bicarbonate solution containing in mM: 130 NaCl, 3.6 KCl, 1.5 $CaCl_2$, 0.5 $MgSO_4$, 0.5 NaH_2PO_4, 2 $NaHCO_3$, 10 HEPES and 0.1% (wt/vol) bovine serum albumin, pH 7.4.[2] Treatments were applied as indicated and photoswitching performed at λ = 340 ± 10 nm using a BMG Fluostar Optima platereader, as above. Insulin concentrations in the supernatant were measured using a Cisbio HTRF assay according to the low-range (sensitive) protocol.

Statistics

Non-multifactorial comparisons were made using Student's t-test. Multifactorial comparisons were made using either one- or two-way ANOVA, or the Kruskal-Wallis test, followed by pairwise comparisons using Bonferonni's or Dunn's tests. Log-transformed concentration-response curves were fitted using non-linear regression and the Hill equation. All analyses were conducted using Graphpad Prism (Graphpad Software) and IgorPro, and results deemed significant at $P<0.05$.

3. *Supplementary Figures and Tables*

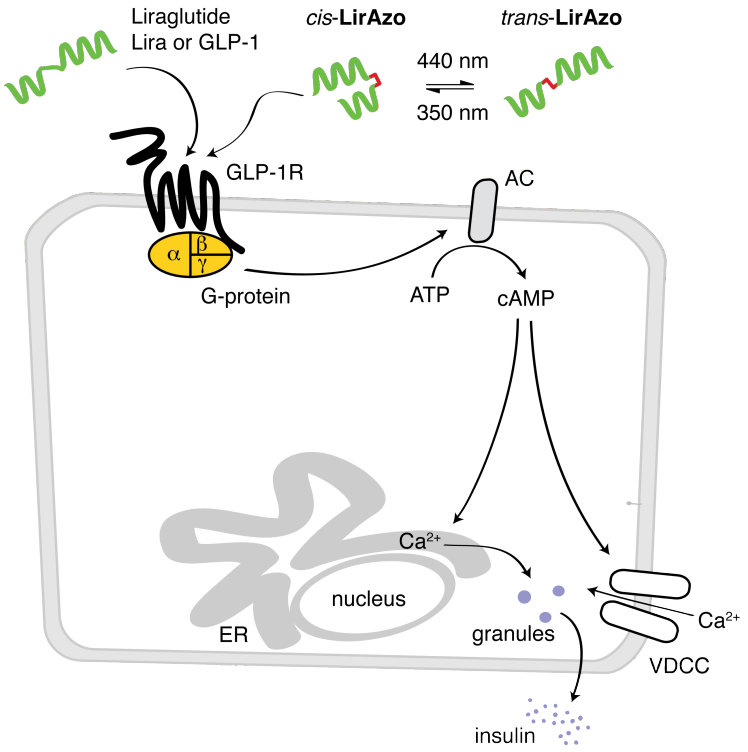

Supplementary Figure 1: GLP-1R signaling and stimulus-secretion coupling in the pancreatic beta-cell.

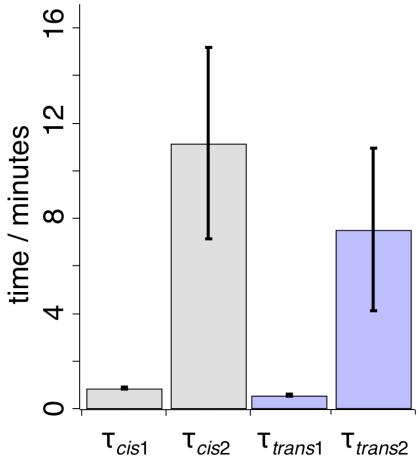

Supplementary Figure 2: LirAzo photoswitching kinetics. *cis*-Isomerization occurs over the minutes timescale (*n* = 4).Values represent mean ± S.D.

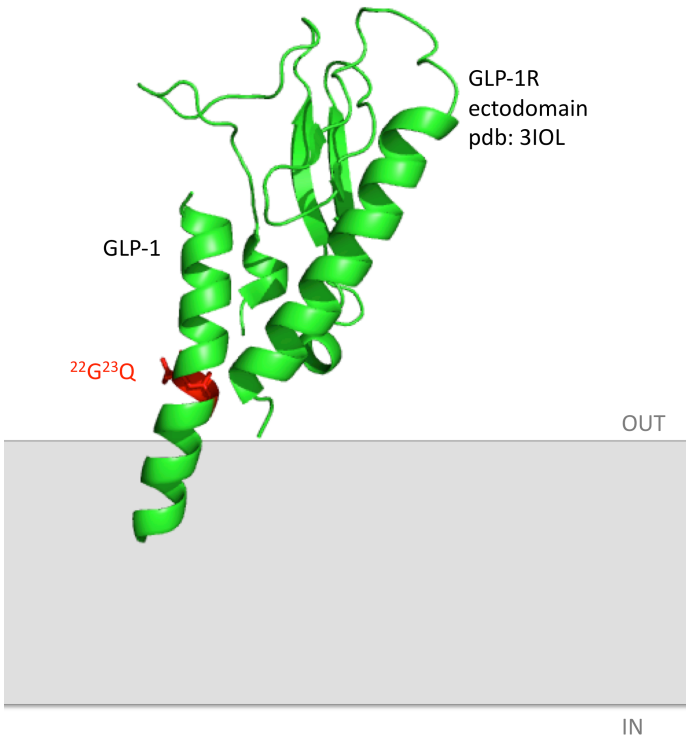

Supplementary Figure 3: GLP-1 bound to the GLP-1R ectodomain (pdb: 3iol)[4] served as an additional model for the design of **LirAzo**. GLP-1 binds to the GLP-1R ectodomain through interactions of ^{22}G-^{37}G. Moreover, the N-terminus is believed to interact with the 7TM domain located in the lipid bilayer. Therefore, we propose that replacement of ^{22}G-^{23}Q (highlighted in red) with AMPP will alter one or both of the helical interactions, leading to divergent class B GPCR signaling through isomer bias. To date, no crystal structure of the full GLP-1R is available. However, the homologous glucagon receptor (GCGR) has been resolved in atomic detail and used to model GLP-1 interactions depicting binding to the 7TM domain.[5] Taken together, a more detailed activation model can only be proposed using an x-ray structure of GLP-1R that highlights the specific interactions with the 7TM domain.

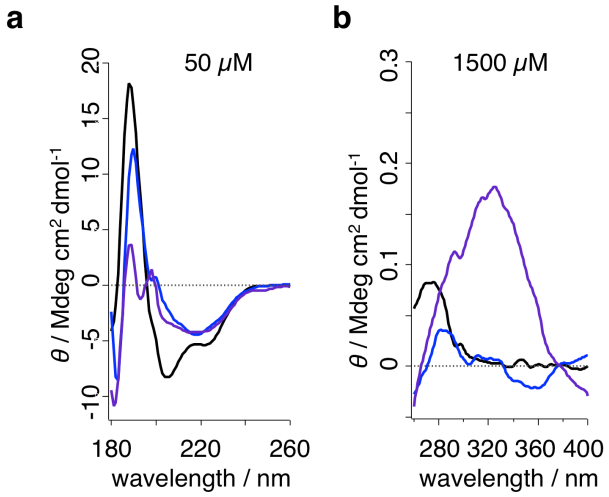

Supplementary Figure 4: CD spectral data of Lira and *cis*-/*trans*-**LirAzo**. a) Far UV spectra and b) Near UV spectra of Lira (black), *trans*-**LirAzo** (blue) and *cis*-**LirAzo** (purple) at 50 µM and 1500 µM concentrations, respectively. Lira exhibits two minima (λ = 205 and 223 nm) and a pronounced rise to a maximum (λ = 188 nm), typical of α-helix possession. Consistent with this, both *cis*-/*trans*-**LirAzo** exhibit minima in the λ = 200-220 nm region. However, whereas *trans*-**LirAzo** displays a maximum at λ = 180 nm, *cis*-**LirAzo** only shows a weak maximum (λ = 189 nm) after a local minimum (λ = 193 nm), consistent with (partial) helix unfolding. Moreover, in the near UV-region, the signal of *cis*-**LirAzo** rises to a maximum (λ = 326 nm) that can be assigned to the *cis*-azobenzene moiety in a chiral environment.

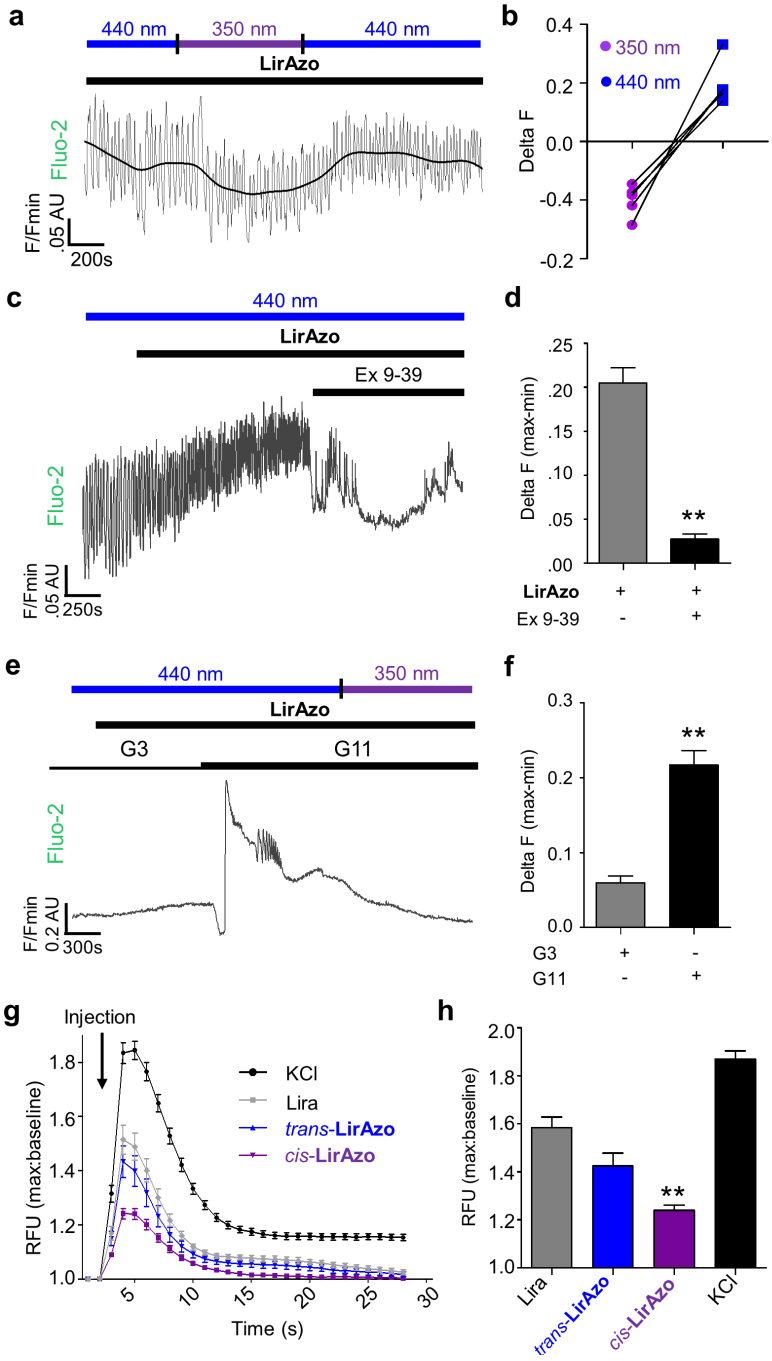

Supplementary Figure 5: Photoswitching of ionic fluxes in beta cells, and GLP-1R- and glucose-dependency. a) Representative trace showing reversible control of GLP-1R signaling and Ca^{2+} levels (*n* = 4 recordings) (smoothed trace shown in black). b) As for a) but before-after plot showing reversal of *cis*-**LirAzo** effects following exposure to blue light to induce *trans*-isomerization (*n* = 4 recordings). c-d) Exendin 9-39 (Ex 9-39) 150 nM abolishes *trans*-**LirAzo**-stimulated Ca^{2+} oscillations (*n* = 9 recordings). e-f) *trans*-**LirAzo** 150 nM is unable to properly stimulate Ca^{2+} rises in the presence of low (non-permissive) glucose concentration (G3; 3 mM glucose) (G11; 11 mM glucose) (*n* = 5 recordings). g-h)

LirAzo allows photoswitching of Ca^{2+} in immortalized MIN6 beta cells subjected to high-throughput assays (*n* = 4 repeats). Lira/**LirAzo** were applied at 150 nM in the presence of permissive (> 8 mM) glucose concentration. **P<0.01 *versus* **LirAzo**/Lira. Values represent mean ± S.E.M.

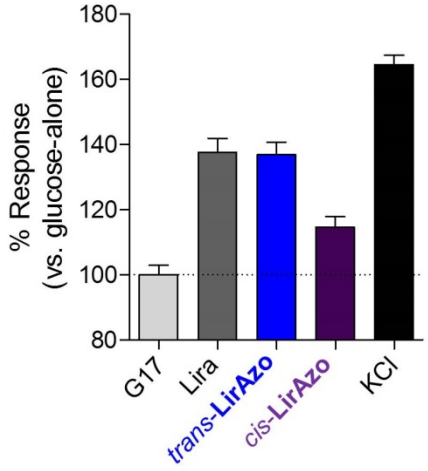

Supplementary Figure 6: LirAzo-stimulated Ca^{2+} rises *versus* control (*i.e.* 17 mM glucose; G17) (KCl, positive control) (*n* = 8).

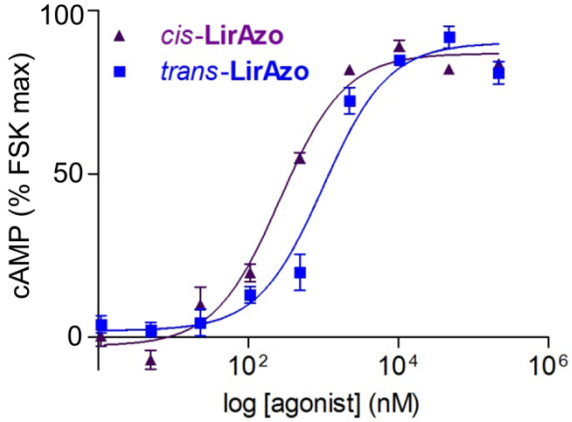

Supplementary Figure 7: Photoswitching of cAMP generation in CHO-GLP-1R cells. Identical to Figure 2d (main text), except showing only cAMP concentration-responses for *cis*- (EC_{50} = 262.0 nM) and *trans*-**LirAzo** (EC_{50} = 993.6 nM) (*n* = 3 repeats) on a contracted x-axis, for clarity. Values represent mean ± S.E.M.

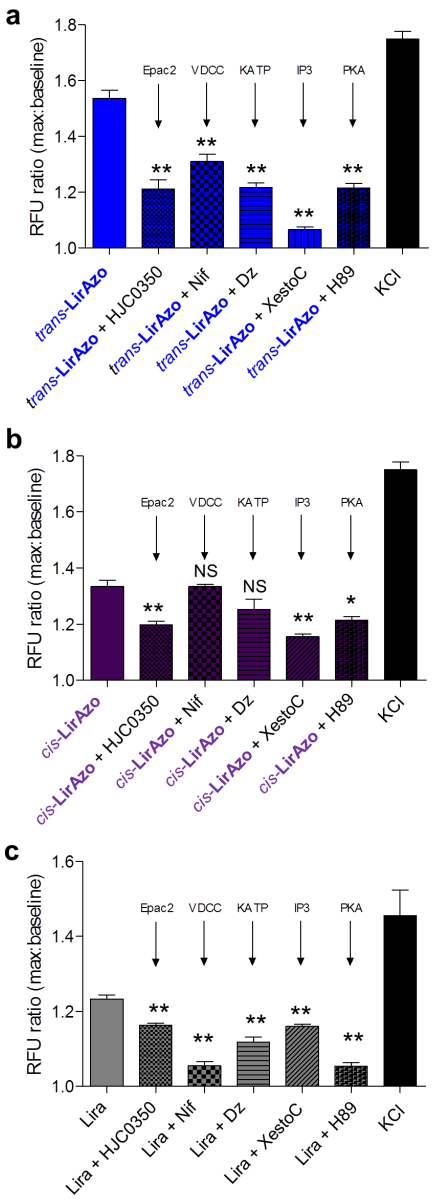

Supplementary Figure 8: Isomer-dependent engagement of beta cell signaling pathways. a) Effects of *trans*-**LirAzo** on cytosolic Ca^{2+} rises in MIN6 beta cells are blocked by antagonists of Epac2 (HJC0350 10 μM), L-type Ca^{2+} channels (Nif, nifedipine 50 μM), K_{ATP} (Dz, diazoxide 150 μM), IP_3R (XestoC, Xestospongin C 10 μM) and PKA (H89, 10 μM) (*n* = 8 repeats). b) As for a), but effects of *cis*-**LirAzo** are only blocked by inhibitors of Epac2, IP_3R and PKA. c) As for a) but Lira positive control showing blockade by all inhibitors. Cells were retained in permissive (> 8 mM) glucose concentration and Lira/**LirAzo** applied at 150 nM. *cis*- and *trans*-**LirAzo** were run in parallel in the same assay, and KCl used as a single positive control for a) and b). *P<0.05, **P<0.01 and NS, non-significant *versus* **LirAzo**-alone. Values represent mean ± S.E.M.

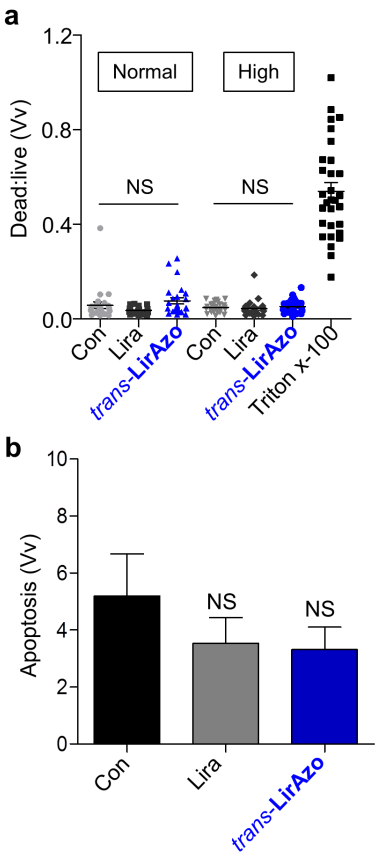

Supplementary Figure 9: LirAzo does not induce cytotoxicity in beta cells. a) Normal (150 nM) and high (2000 nM) concentrations of LirAzo do not alter islet viability (Triton X-100; positive control) (n = 20-25 islets) (Con, control). b) Lira and *trans*-**LirAzo** do not induce islet cell apoptosis under normal conditions (*i.e.* 11 mM glucose-only), as determined using TUNEL staining (*n* = 8-9 islets). NS, Non-significant *versus* control (Con). Values represent mean ± S.E.M.

Supplementary Table 1: Coupling conditions for peptide synthesis

compound	step	Lira			**LirAzo**		
		t [s]	p [W]	T [°C]	t [s]	p [W]	T [°C]
FmocGlyOH	1	480	23	75	480	23	75
FmocArg(Pbf)OH	1	1500	0	r.t.	1500	0	r.t.
	2	300	25	75	300	25	75
FmocGlyOH	1	480	23	75	480	23	75
FmocLys(Boc)OH	1	480	23	75	480	23	75
FmocValOH	1	480	23	75	480	23	75
FmocLeuOH	1	480	23	75	480	23	75
FmocTrp(Boc)OH	1	480	23	75	480	23	75
FmocAlaOH	1	480	23	75	480	23	75
FmocIleOH	1	480	23	75	480	23	75
FmocPheOH	1	480	23	75	480	23	75
FmocGlu(*t*Bu)OH	1	480	23	75	480	23	75
FmocLys(Boc)OH	1	480	23	75	480	23	75
FmocAlaOH	1	480	23	75	480	23	75
FmocAlaOH	1	480	23	75	480	23	75
FmocGln(Trt)OH	1	480	23	75			
FmocGlyOH	1	480	23	75			
FmocAMPPOH	1				300	0	r.t.
	2				1800	23	75
FmocGlu(O*t*Bu)OH	1	480	23	75	480	23	75
FmocLeuOH	1	480	23	75	480	23	75
FmocTyr(*t*Bu)OH	1	480	23	75	480	23	75
FmocSer(*t*Bu)OH	1	480	23	75	480	23	75

FmocSer(*t*Bu)OH	1	480	23	75	480	23	75
FmocValOH	1	480	23	75	480	23	75
FmocAsn(Trt)OH	1	480	23	75	480	23	75
FmocSer(*t*Bu)OH	1	480	23	75	480	23	75
FmocThr(*t*Bu)OH	1	480	23	75	480	23	75
FmocPheOH	1	480	23	75	480	23	75
FmocThr(*t*Bu)OH	1	480	23	75	480	23	75
FmocGlyOH	1	480	23	75	480	23	75
FmocGlu(*t*Bu)OH	1	480	23	75	480	23	75
FmocAlaOH	1	480	23	75	480	23	75
FmocHis(Trt)OH	1 2	120 240	0 23	r.t. 50	120 240	0 23	r.t. 50

Supplementary Table 2: LirAzo photoswitching kinetics

LirAzo	τ_1 (sec)	τ_2 (min)
cis	51.0±2.4	11.1±4.0
trans	32.3±1.6	7.5±3.4

Supplementary Table 3: H and C atom chemical shift data of *cis/trans*-AMPP in *trans*- and *cis*-**LirAzo** peptides.

	trans-**LirAzo**		*cis*-**LirAzo**	
AMPP	H [ppm]	C [ppm]	H [ppm]	C [ppm]
2	4.46, 4.38	45.2	4.26, 4.19	44.9
4	7.72	125.5	6.82	122.5
6	7.64	123.6	6.48	120.7
7	7.41	131.6	7.22	129.3
8	7.36	132.8	7.06	129.5
12	7.79	125.0	6.90	124.4
14	7.44	134.3	7.12	131.1
15	7.45	131.9	7.11	131.5
16	7.70	123.8	6.58	120.9
17	3.87	44.0	3.57, 3.45	43.8

Supplementary Table 4: EC_{50} values for cAMP generation in CHO-GLP-1R cells. *P<0.03 and $^{\$}$P<0.34 *versus cis*-**LirAzo**(Lira; liraglutide) (Student's t-test). 95% Confidence intervals are shown in brackets.

	cis-**LirAzo**	*trans*-**LirAzo**	Lira
EC_{50} (nM)	262.0 (199.5 to 344.1)	993.6* (681.6 to 1448)	98.93$^{\$}$ (69.14 to 141.5)

4. References

[1] a) A. Aemissegger, V. Krautler, W. F. van Gunsteren, D. Hilvert, *J. Am. Chem. Soc.* **2005**, *127*, 2929-2936; b) T. Podewin, M. S. Rampp, I. Turkanovic, K. L. Karaghiosoff, W. Zinth, A. Hoffmann-Röder, *Chem. Commun.* **2015**, *51*, 4001-4004.

[2] M. A. Ravier, G. A. Rutter, *Diabetes* **2005**, *54*, 1789-1797.

[3] a) D. J. Hodson, R. K. Mitchell, E. A. Bellomo, G. Sun, L. Vinet, P. Meda, D. Li, W. H. Li, M. Bugliani, P. Marchetti, D. Bosco, L. Piemonti, P. Johnson, S. J. Hughes, G. A. Rutter, *J. Clin. Invest.* **2013**, *123*, 4182-4194; b) D. J. Hodson, R. K. Mitchell, L. Marselli, T. J. Pullen, S. Gimeno Brias, F. Semplici, K. L. Everett, D. M. Cooper, M. Bugliani, P. Marchetti, V. Lavallard, D. Bosco, L. Piemonti, P. R. Johnson, S. J. Hughes, D. Li, W. H. Li, A. M. Shapiro, G. A. Rutter, *Diabetes* **2014**, *63*, 3009-3021.

[4] C. R. Underwood, P. Garibay, L. B. Knudsen, S. Hastrup, G. H. Peters, R. Rudolph, S. Reedtz-Runge, *J. Biol. Chem.* **2010**, *285*, 723-730.

[5] F. Y. Siu, M. He, C. de Graaf, G. W. Han, D. Yang, Z. Zhang, C. Zhou, Q. Xu, D. Wacker, J. S. Joseph, W. Liu, J. Lau, V. Cherezov, V. Katritch, M. W. Wang, R. C. Stevens, *Nature* **2013**, *499*, 444-449.